applied sciences

MDPI

Article

Effect of Slag Particle Size on Fracture Toughness of Concrete

Chung-Ho Huang [1], Chung-Hao Wu [2,*], Shu-Ken Lin [3] and Tsong Yen [3]

1 Department of Civil Engineering, National Taipei University of Technology, Taipei City 106, Taiwan; cdewsx.hch@gmail.com
2 Department of Civil Engineering, Chienkuo Technology University, Changhua City 500, Taiwan
3 Department of Civil Engineering, National Chung-Hsing University, No.145, Xingda Road, Taichung 402, Taiwan; sklin@nchu.edu.tw (S.-K.L.); tyen@dragon.nchu.edu.tw (T.Y.)
* Correspondence: chw@ctu.edu.tw; Tel.: +886-4-7111111 (ext. 3428)

Received: 1 February 2019; Accepted: 20 February 2019; Published: 25 February 2019

Abstract: The effects of particle size of ground granulated blast furnace slag (GGBS) on the fracture energy, critical stress intensity, and strength of concrete are experimentally studied. Three fineness levels of GGBS of 4000, 5000, 6000 cm^2/g were used. In addition to the control mixture without slag, two slag replacement levels of 20% and 40% by weight of the cementitious material were selected for preparing the concrete mixtures. The control mixture was designed to have a target compressive strength at 28 days of 62 MPa, while the water to cementitious material ratio was selected as 0.35 for all mixtures. Test results indicate that using finer slag in concrete may improve the filling effect and the reactivity of slag, resulting in a larger strength enhancement. The compressive strength of slag concrete was found to increase in conjunction with the fineness level of the slag presented in the mixture. Use of finer slag presents a beneficial effect on the fracture energy (G_F) of concrete, even at an early age, and attains a higher increment of G_F at later age (56 days). This implicates that the finer slag can have a unique effect on the enhancement of the fracture resistance of concrete. The test results of the critical stress intensity factor ($K^S{}_{IC}$) of the slag concretes have a similar tendency as that of the fracture energy, indicating that the finer slag may present an increase in the fracture toughness of concrete.

Keywords: fracture toughness; blast furnace slag; particle size; compressive strength; concrete

1. Introduction

Ground granulated blast furnace slag (GGBS) is a byproduct of iron making, which is produced by water quenching of molten blast furnace slag that turns out to be a glassy material [1]. It is ground to improve the reactivity during cement hydration. GGBS is one such supplementary material which can be used as a cementitious ingredient in either cement or concrete composites. Research to date suggests that the supplementary cementitious materials improve many of the performance characteristics of concrete, such as strength, workability, and corrosion resistance [2,3]. Some of the effective parameters like chemical composition, fineness, and hydraulic reactivity have been carefully examined by many earlier studies [4]. Among these, the reactive glass content and fineness of GGBS alone will influence the cementitious/pozzolanic efficiency or its reactivity in concrete composite significantly.

It is generally agreed that the use of fine GGBS improves the properties of concrete. K. Tan and X. Pu [5] investigated the effect of finely ground GGBS on the compressive strength of concrete. Test results showed that incorporating 20% finely ground GGBS can significantly increase the strength after 3 days. Mantel [6] reported that the slag activity depends on the particle size distribution (fineness) of slag and the cement used and showed that this ranges from 62%–115% at 28 days. In addition, the investigation of Yűksel et al. [7] reported that the increase in fineness of GGBS improves compressive strength due to the pozzolanic reaction causing a reduction in permeability, signifying that finer slag can provide higher resistance against deteriorations from chemical or physical attacks.

The traditional properties, such as compressive strength, have been assessed to be in close relation to the pore characteristic and interfacial transition zone (ITZ) of concrete. The test results of Duan, Gao, and Tan et al. [5,8,9] show that mineral admixtures have a positive impact on pore refinement and ITZ enhancement, especially at later curing stages. The development of compressive strength is significantly related to the evolution of ITZ and the pore structure. In fact, the cementitious and pozzolanic behavior of GGBS is essentially similar to that of high-calcium fly ash. Previous reports [5,9–11] have primarily indicated that increasing the fineness of fly ash and slag may increase the strength and durability of concrete attributed to the microcracking resistance of cement paste, particularly in ITZ.

The interfacial transition zone in concrete that is often modeled as a three-phase material is represented as the third phase [12]. Existing as a thin shell around larger aggregate, the ITZ is generally weaker than either of the two main components, the hydrated cement paste, and aggregate, of concrete. The ITZ has less crack resistance, and accordingly, the factor occurs preferentially. A major factor responsible for the poor strength of the ITZ is the presence of microcracks. Much of the physical nature of the response of concrete under loading can be described in terms of microcracks that can be observed at relatively low magnification. Cracking in concrete is mostly due to the tensile stress that occurs under load or environmental changes. As such, the failure of concrete in tension is governed by the microcracking, associated particularly with the ITZ [13,14].

The tensile strength of concrete is a very essential property. Not only the tensile strength but also the behavior at the tensile fracture is of importance, particularly the toughness. When concrete fails in tension, its behavior is characterized by both the peak stress and the energy required to fully generate a crack. Fracture mechanics could in principle be a suitable basis for analyzing the tensile toughness of concrete [15]. The defects and the stress concentration are the main factors causing failure. Concrete that exhibits defects or is subjected to stress concentrations easily cracks and results in a reduction of strength. It is important to identify the fracture behavior and toughness for widely used high-performance concrete that normally incorporates slag or fly ash [16,17].

Because of the non-homogeneous characteristics of concrete, its fracture behavior is quite complicated. It was proved that the methods developed in conventional fracture mechanics are unsuitable for the analysis of the influence of fracture toughness on the behavior of concrete structures [15]. Many theoretical models have been developed to make such an analysis possible. Among them, three well-known models are the fictitious crack model, the crack band model, and the two-parameter fracture model. By means of numerical techniques, for example, in the finite element method, it is possible using these models to make a theoretical analysis for the development of the damage zone and the complete behavior of the structure. As for the fracture mechanics of concrete, RILEM has put forward several methods to determine the fracture properties and parameters of concrete [18]. Hillerborg [15] determine the fracture energy according to the fictitious crack model. Jeng and Shah [19] used the two-parameter fracture model to determine the critical stress intensity factor.

A number of past studies on the concrete containing GGBS have been conducted, mainly dealing with the influence of the fineness of slag on the strength and durability of concrete. More rarely, investigations were conducted on the fracture behaviors of concrete incorporating finer GGBS. Consequently, there is a need for exploring the effects of the particle size of GGBS on the fracture properties of concrete. This study experimented using the three-point bend test to analyze the fracture energy and the critical stress intensity factor for evaluating the fracture mechanics or fracture toughness of concrete containing finer GGBS.

2. Research Significance

Laboratory investigations have shown that when the slag particle size is reduced, its mechanical performance in concrete is improved. The finer slag with the larger surface area has an intensive reaction which may lead to higher enhancement of the strength, the fracture energy, and the critical stress intensity factor of concrete. Other than the research by Jensen and Hansen [20], who observed a dependence of the fracture energy on the aggregate type and independence from the compressive strength of concrete, this study found that an increase in concrete compressive strength of 10% resulted in an increase in fracture energy of around 18%.

3. Experimental Details

3.1. Materials

The materials used included a Type I Portland cement, river sand, crushed coarse aggregate with a maximum size of 10mm, a naphthalene-sulfonate-based superplasticizer, and GGBS of three fineness levels. The chemical composition of cement and GGBS are presented in Table 1. Three different fineness levels of GGBS of 4000, 5000, and 6000 cm^2/g with a specific gravity of 2.85 were selected in this study.

Table 1. Chemical analysis of cement and ground granulated blast furnace slag (GGBS).

Chemical Analysis (%)	SiO_2	Al_2O_3	Fe_2O_3	CaO	MgO	SO_3	Na_2O	K_2O	LOI
Cement	20.9	5.62	3.21	63.6	2.52	2.16	0.27	0.52	0.92
GGBS	33.1	15.6	0.33	40.7	7.7	0.1	-	-	0.12

3.2. Mixture Proportions

Seven mixtures were prepared for testing in this research: A reference mixture (R0) without GGBS and six slag mixtures, designated as S4R2, S4R4, S5R2, S5R4, S6R2, and S6R4. S4, S5, and S6 refer to slag fineness of 4000, 5000 and 6000 cm^2/g, respectively. R2 and R4 refer to the replacement ratios of 20% and 40%, respectively, by weight of the cementitious material. The water to cementitious material ratio (w/cm) was kept at 0.35 for all mixtures. All concretes were designed to have a target compressive strength level at 28 days of 62 MPa. The dosage of superplasticizer was adjusted to produce a designed slump of 250 ± 20 mm and a slump flow of 600 ± 50 mm for all mixtures. The mixture proportions are shown in Table 2.

Table 2. Mixture proportions and properties of fresh concrete.

Mixture No.	w/cm	Water	Cement	Slag	Sand	Aggregate	SP.	Slump	Slump Flow
		kg						mm	mm
R0	0.35	182	520	0	850	783	8.1	230	625
S4R2			416	104	850	803	7.5	230	625
S4R4			312	208	870	773	6.8	265	580
S5R2			416	104	850	803	7.8	250	620
S5R4			312	208	860	783	6.8	255	610
S6R2			416	104	850	803	7.5	255	585
S6R4			312	208	840	793	7.0	235	580

3.3. Specimen Fabrication

Cylinder specimens (ψ100 × 200 mm) were cast from each mixture for compression testing; three cylinders each for testing at 4 ages (7, 14, 28, 56 days). Prism specimens with diminution of 50 × 50 × 650 mm and 80 × 150 × 700 mm were cast for the determination of fracture energy (G_F) and the critical stress intensity factor (K^S_{IC}), respectively. Four specimens were fabricated for each mixture that tested the two specimens at 2 ages (14 and 56 days). The specimens and concrete mixtures were prepared in accordance with ASTM C192. After casting, test specimens were covered with plastic sheets and left in the casting room for 24 h. They were then demolded and put into a 100% RH moist-curing room at about 23 °C until time for testing. One day before testing, the fracture energy specimen and the critical stress intensity factor specimen, as shown in Figures 1 and 2, were prepared by cutting a notches 25 mm deep by 2 mm width and 50 mm deep by 2 mm width, respectively, at the middle of the beam specimens.

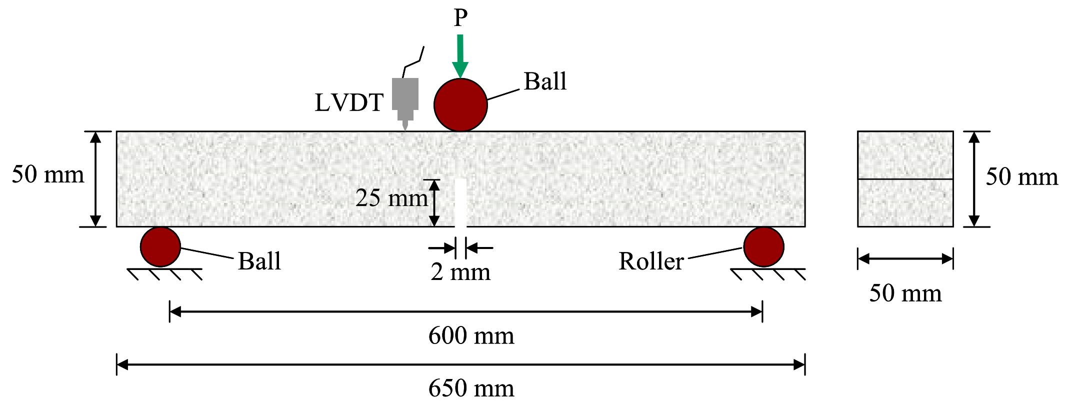

Figure 1. The test set up for G_F–determination.

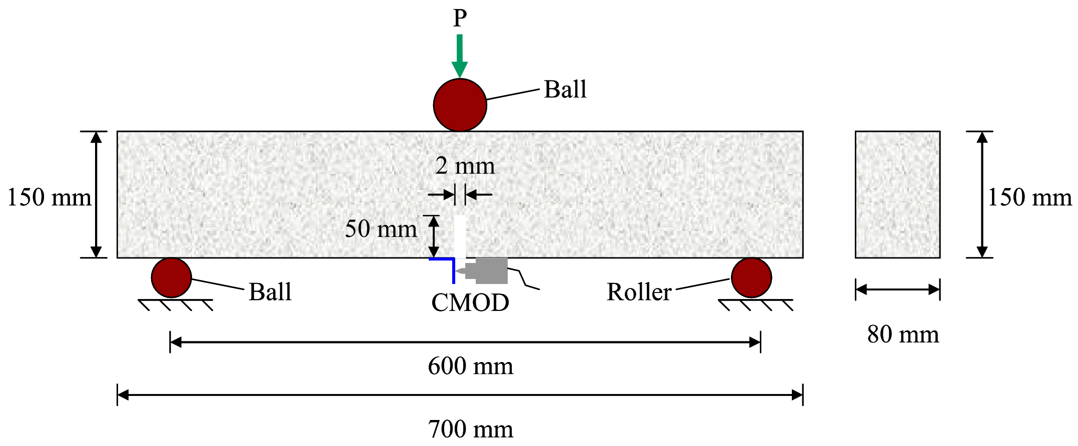

Figure 2. The test set up for K^S_{IC}-determination.

3.4. Testing Procedure

The compression test was carried out in accordance with ASTM C39. The three-point bending test was performed on the notched beam as follows to determine the G_F and K^S_{IC}:

3.4.1. The Test for Determining G_F

The fracture energy test followed the guidelines established by RILEM [21] using a closed-loop testing machine. The testing arrangement is shown in Figure 1. A linear variable differential transformer (LVDT) was installed at mid-span of the beam to measure the deflection. The loading velocity was chosen so that the maximum load was reached 30 s after the loading started. The loading rate selected was 0.25 mm/min. A load-deflection (F-δ) curve was then plotted, with the energy "W_0" representing the area under the curve. The G_F (N-m) can be calculated using the following expression [15,19]:

$$G_F = W_0 + mg\frac{\delta_0}{A} \tag{1}$$

where W_0 = area under the load-deflection curve (N-m);

m = mass of the beam between the supports (kg);
g = acceleration due to gravity;
δ_0 = final deflection of the beam (m);
A = cross-sectional area of the beam above the notch (m^2).

3.4.2. Test for Determining K^S_{IC}

The test for the determination of K^S_{IC} followed the test method suggested by Jenq and Shah [19] using a closed-loop testing machine under crack mouth opening displacement (CMOD) control. The test setup is shown in Figure 2. A clip gauge was used to measure the CMOD. The CMOD and the applied load were recorded continuously during the test. The test procedure included two steps of loading and unloading. The first step was started from loading until the peak load was reached; the applied load was manually reduced (also termed unloading) when the load passed the maximum load and was about 95% of the peak load. When the applied load was reduced to zero, reloading was applied. Each loading and unloading cycle was finished in about 1 min. Only one cycle of loading-unloading was required for the test. The K^S_{IC} is calculated using the following equation:

$$K^S_{IC} = \frac{3P_{\max}S}{2bd^2}\sqrt{(\pi\alpha_c)}F(\alpha) \tag{2}$$

in which,

$$F(\alpha) = 1.99 - \frac{\alpha(1-\alpha)(2.15 - 3.93\alpha + 2.7\alpha^2)}{\sqrt{\pi}(1+2\alpha)(1-\alpha)^{3/2}} \tag{3}$$

where P_{max} = the measured maximum load (N);
S = the span of the beam; b = beam width; d = beam depth;
α_c = critical effective crack length;
$\alpha = \alpha_c/d$.

4. Results and Discussion

4.1. Compressive Strength

Compressive strength was determined at the ages of 7, 14, 28 and 56 days on concrete stored under moist-curing condition. The results are shown in Table 3. It is seen that all mixtures were proportioned to have equivalent workability and target strengths of 62 MPa at the age of 28 days. This was generally achieved except for in mixtures S4R2 and S4R4. In this case, the strength equivalence was achieved at the age of 56 days, which was also exceeded by that of the reference mixture (R0).

The development of compressive strength for each concrete mixture is shown in Figure 3. At early ages (7 days), as expected, the reference mixture without slag exhibited higher strength than the other slag mixtures. The early strength gain of the reference mixture was superior to that of the slag mixtures, indicating that replacing any amount of cement with GGBS of various fineness will reduce the strength of concrete. Moreover, the concrete incorporating more slag (40%) displayed lower strength at an early age than that with less slag content (20%). However, the curve slope of the slag mixtures in Figure 3 tends to be steeper than that of the reference mixture at later ages. In other words, the strength increment versus age for the slag mixtures is obviously larger than that of the reference mixture. Consequently, the strength of each slag mixture exceeds that of the reference mixture at the age of 56 days.

On the other hand, it can be found from Table 3 that under the same replacement ratio (20% and 40%) of slag, the mixtures S6R2 and S6R4 presented the highest strengths at an early age (7 days), followed by S5R2 and S5R4, and the S4R2 and S4R4 mixtures are the lowest. This is due to the fact that incorporating finer slag into concrete may fill the micro-voids much better, exhibit higher reactivity and producing higher packing density, resulting in a larger strength enhancement. In addition, a beneficial effect of the fineness of slag on concrete strength can be seen in Figure 4; the compressive strength of the slag concrete increases as the fineness level of the slag incorporated into the mixture increases for each age and various slag replacement ratios. It is also found in Table 3 that there are significant strength gains from 7–28 days and again from 28–56 days for the mixture containing finer slag. For example, the strength increment of the mixtures S6R2 and S6R4 that contain finer slag displayed an increase rate from 100% at 7 days to 121.8% and 122.7% at 28 days, and 125.5% and 128.9% at 56 days, respectively. These are obviously larger than the corresponding mixtures of S4R2 and S4R4 that increased from 100% at 7 days to 114.9% and 115.1% at 28 days, and 124.2% and 126.2% at 56 days, respectively. At 28 days, the strength of the finer-slag concrete is shown consistently to exceed that of the reference concrete, except in the mixtures of S4R2 and S4R4. This is particularly significant considering that the cement replacement of finer slag in each case is up to 40%. In addition, the highest strength achieved at 56 days was 70.5 MPa for the mixture S6R4 with 40% slag replacement, while the strength obtained for the corresponding reference mixture was a relatively lower value of 65.5 MPa.

Table 3. The compressive strength of concrete cylinders.

Mixture No.	w/cm	Compressive Strength (MPa)			
		7 Days	14 Days	28 Days	56 Days
S0	0.35	56.2 (100%)	60.7 (108.0%)	63.2 (112.5%)	65.5 (116.5%)
S4R2		54.5 (100%)	59.2 (108.6%)	62.6 (114.9%)	67.7 (124.2%)
S4R4		53.0 (100%)	58.7 (110.8%)	61.0 (115.1%)	66.9 (126.2%)
S5R2		55.0 (100%)	60.1 (109.3%)	65.5 (119.1%)	69.1 (125.6%)
S5R4		54.2 (100%)	59.5 (109.8%)	64.8 (119.6%)	68.4 (126.2%)
S6R2		56.0 (100%)	62.3 (111.3%)	68.2 (121.8%)	70.3 (125.5%)
S6R4		54.7 (100%)	61.0 (111.5%)	67.1 (122.7%)	70.5 (128.9%)

* Average value of three specimens

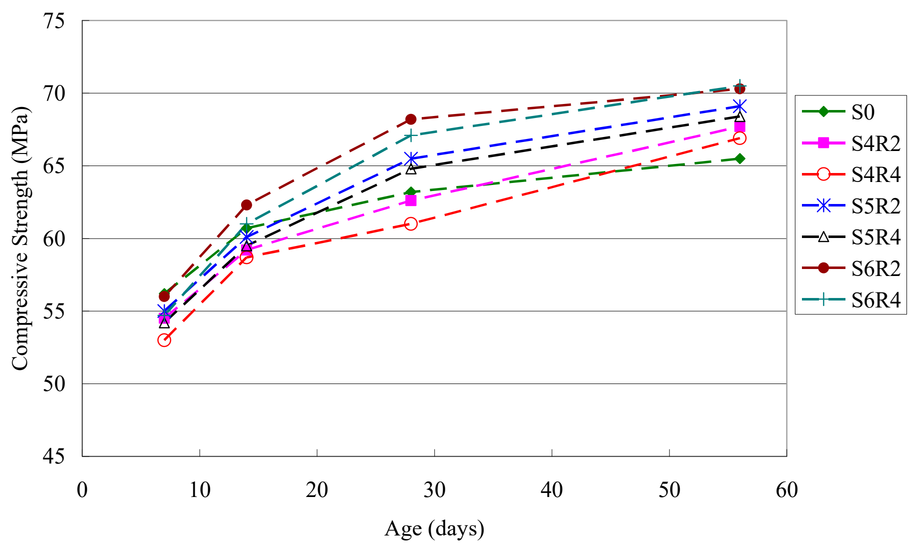

Figure 3. Compressive strength development for cylindrical specimens.

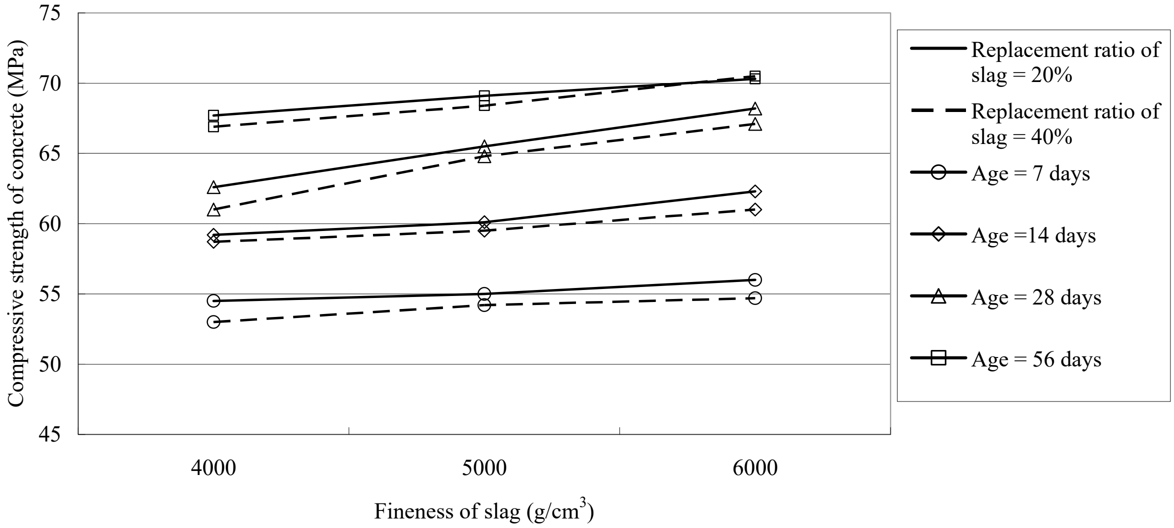

Figure 4. The average compressive strength of slag concrete versus the fineness of ground granulated blast furnace slag (GGBS).

4.2. Fracture Energy

In this research, fracture energy (G_F) was determined using a notched beam in a three-point bending test. Load-deflection curves were plotted from the tests. The energy absorbed in the test to failure is represented by the area below the load-deflection curve for the specimen. The area represents the fracture energy per unit area of the fracture surface. The G_F was calculated using Equation (1). Concrete specimens were tested at 14 and 56 days. Results are presented in Table 4. At earlier ages (14 days), the G_F values of each slag mixture are mostly less than that of the reference mixture, except slag mixture S6R2. In addition, the concrete containing more slag (40%) presented smaller G_F than that with less slag content (20%) for various ages. Nevertheless, the presence of the finer slag has a beneficial effect on the G_F of concrete. As shown in Figure 5, increasing the fineness level of slag leads to an increase of the G_F value of concrete. Even at an earlier age of 14 days, the G_F value of the mixture with finer slag (S6R4) is in turn higher than that of the mixtures S5R4 and S4R4 for a similar slag replacement ratio of 40%. This implies that although the pozzolanic reaction of slag does not yet fully occur at early ages, the superior filling effect and more active hydration reaction of the finer slag can increase the density of concrete, resulting in an increased fracture resistance. After 56 days, the G_F value of the slag mixtures almost exceeds that of the reference mixture. In addition, it is also found in Table 4 that the increment of fracture energy for each slag concrete from 14 days to 56 days is attained by 18–24%, which is much higher than that of reference concrete (10.1%). This signifies that, during the period, the pozzolanic reaction of slag activates, associating with the filling effect to enhance the fracture toughness of the slag concrete.

Table 4. Fracture energy of the concrete.

Mixture No.	Compressive Strength (MPa)		Fracture Energy (N/m)		
	14 Days	56 Days	14 Days	56 Days	Increment N/m (%)
S0	60.7	65.5	74.3	81.8	7.5 (10.1)
S4R2	59.2	67.7	71.2	84.5	13.3 (18.7)
S4R4	58.7	66.9	65.7	78.4	12.7 (19.3)
S5R2	60.1	69.1	72.1	89.1	17.0 (23.5)
S5R4	59.5	68.4	69.8	85.3	15.5 (22.2)
S6R2	62.3	70.3	76.5	94.6	18.1 (23.7)
S6R4	61.0	70.5	73.9	92.1	18.2 (24.6)

* Average value of two specimens

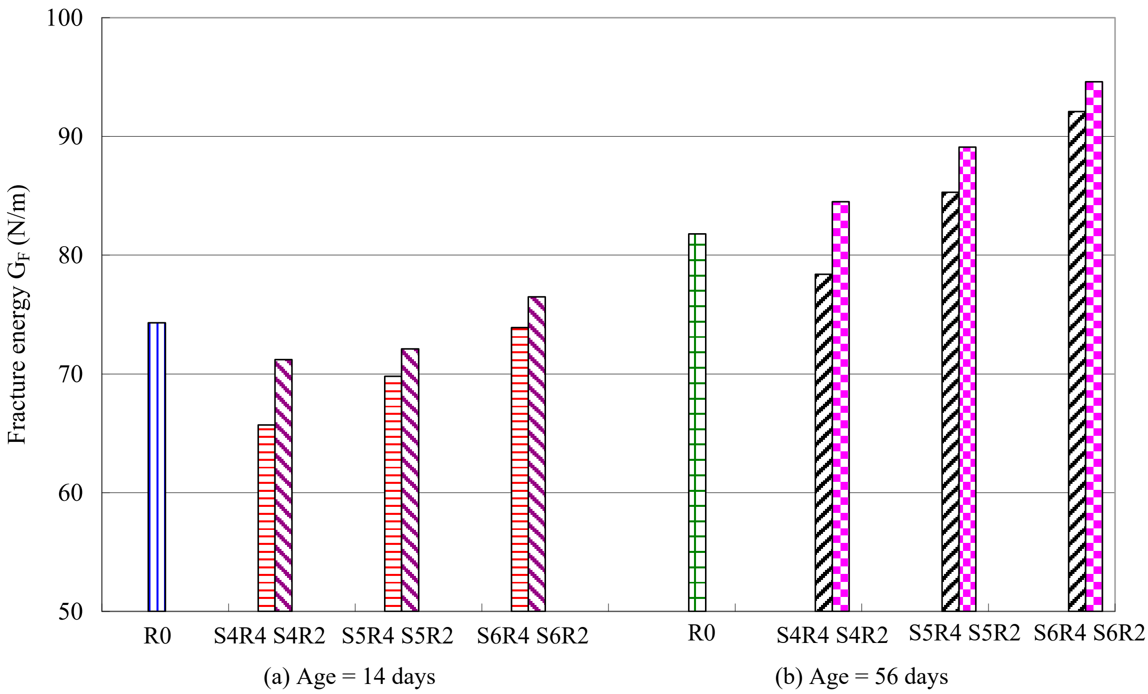

Figure 5. Fracture energy for concretes with various fineness levels and replacement ratios of slag at ages of 14 days and 56 days.

Figure 6 compares fracture energy with the compressive strength of all slag concretes in the study. The G_F is found to increase in conjunction with the compressive strength. This compares the trend favorably with the studies by Giaccio [22], Gettu [23], and Xie [24]. Nevertheless, the other studies observed smaller increases in G_F with the increases in the compressive strength of high-strength concrete. Giaccio, Rocco, and Zerbino [22] found that G_F increased as compressive strength increased, but only at a fraction of the rate. Getta, Bažant, and Kerr [23] reported that an increase in compressive strength of 160% resulted in an increase in G_F of only 12%. Xie, Elwi, and MacGregor [24] found that increases in compressive strength of 29% and 35% resulted in a G_F increase of 11% and 13%, respectively. In this study, an increase in compressive strength of 10% resulted in a larger increase in G_F of around 18%. This implicates the unique effect of using finer slag on the enhancement of the fracture resistance of concrete.

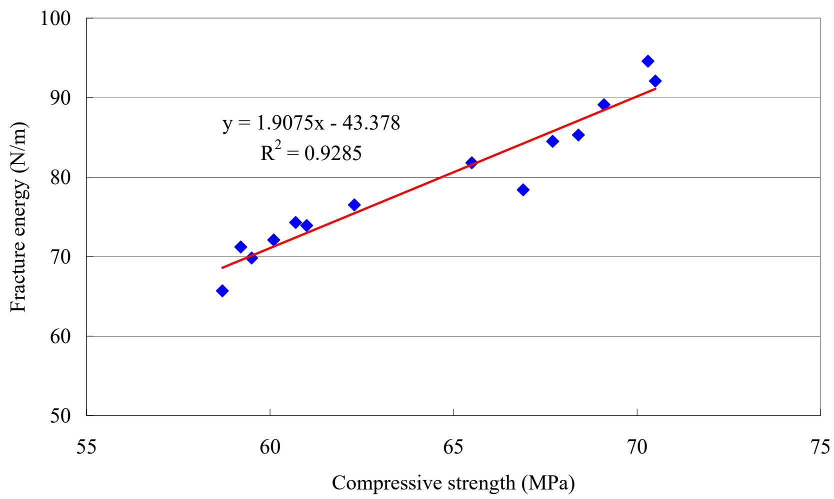

Figure 6. Fracture energy versus compressive strength for slag concretes.

4.3. Critical Stress Intensity Factor

The critical stress intensity factor (K^S_{IC}) was experimentally determined with a notch beam in a three-point bend test using a closed-loop testing machine under the crack mouth opening displacement control. Load-CMOD curves were plotted from the tests. The K^S_{IC} was calculated using Equation (2). Concrete specimens were tested at 14 and 56 days. Table 5 summarizes the results. It shows that the related tendency of the K^S_{IC} of concrete is similar to that of the G_F. At an early age (14 days), the K^S_{IC} values of slag concrete are less that of the reference concrete (R0), but exceed that of R0 after 56 days. This implies that the additional pozzolanic reaction of slag with $Ca(OH)_2$ in concrete becomes active during the period between 14 days and 56 days, which leads to the enhancement of K^S_{IC} of the slag concretes. Moreover, it is seen that the concrete incorporating more slag (40%) presented a lower KSIC value than that with less slag content (20%) for various ages. On the other hand, the concrete containing finer slag can exhibit larger K^S_{IC} values. It can be found from Figure 7 that the increase of the fineness level of the slag leads to an increase in the K^S_{IC} value of concrete for various ages. In other words, the K^S_{IC} value of the mixture with finer slag (S6R2) is in turn higher than those of S5R2 and S4R2 for the similar slag replacement ratio of 20%. Also, the K^S_{IC} of S6R4 > S5R4 > S4R4 for the similar slag replacement ratio of 40%. The reason for this result is that the finer slag particle has a larger surface area, presenting a more active pozzolanic reaction, thus resulting in an increase of strength and fracture toughness.

Table 5. Critical stress intensity factor of the concrete.

Mixture No.	Compressive Strength (MPa)		Critical Stress Intensity Factor ($MPa \times m^{0.5}$)	
	14 Days	56 Days	14 Days	56 Days
S0	60.7	65.5	0.248	0.261
S4R2	59.2	67.7	0.246	0.276
S4R4	58.7	66.9	0.239	0.265
S5R2	60.1	69.1	0.247	0.282
S5R4	59.5	68.4	0.241	0.278
S6R2	62.3	70.3	0.252	0.286
S6R4	61.0	70.5	0.244	0.280

* Average value of two specimens.

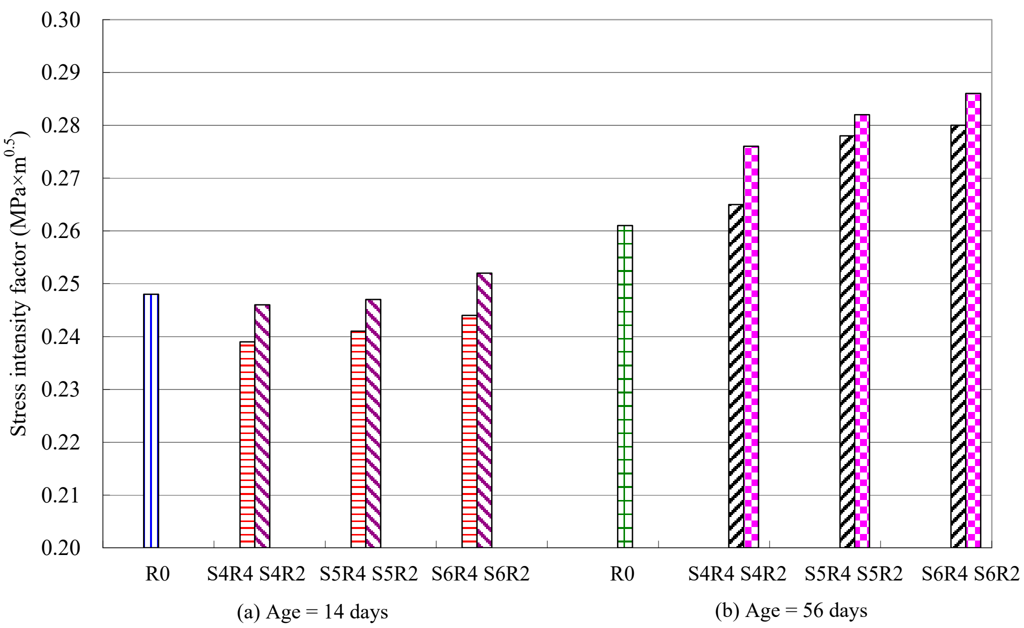

Figure 7. The stress intensity factor for concretes with various fineness levels and replacement ratios of slag at the ages of 14 days and 56 days.

Figure 8 compares the critical stress intensity factor with compressive strength for all slag-concrete specimens in the study. As shown in the figure, the two values of stress are nearly linearly related. The relationships shown in Figure 8 are significant because, based on the close relationship between the particle size of slag and compressive strength (Figure 4), the critical stress intensity factor will increase with the increase of the fineness level of the slag.

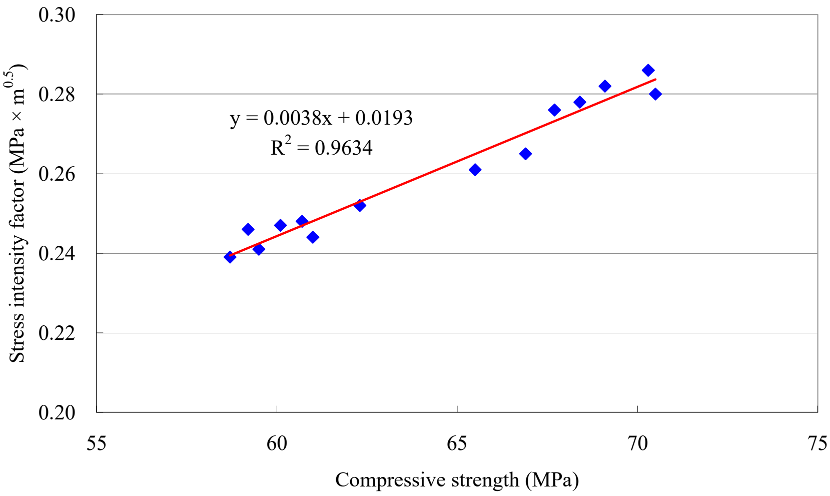

Figure 8. Critical stress intensity factor versus compressive strength for slag concretes.

5. Conclusions

The following conclusions were made based on the experimental results and the findings of the study:

1. The filling effect and the reactivity of slag can be improved by reducing its particle size. Incorporating finer slag into concrete may lead to larger early strength gains and larger strength increments of the concrete at later ages. The compressive strength of slag concrete was found to increase in conjunction with the fineness level of the slag incorporated into the mixture.
2. The use of finer slag presents a beneficial effect on the fracture energy (G_F) of concrete, even at early ages (14 days), due to superior filling effect. Increasing the fineness level of the incorporated slag leads to an increase of the G_F value of concrete or an enhanced fracture toughness.
3. The increment of the fracture energy of all the slag concretes measured in this study from 14–56 days was attained by 18–24%, which is found much higher than that of reference concrete (10.1%), and accordingly, the G_F of the slag mixtures at 56 days almost exceeds that of the reference mixture.
4. An increase in compressive strength of slag concrete of 10% resulted in a fracture energy increase of around 18%. This raise rate is significantly higher than that previously found in high-strength concretes without slag, indicating that use of the finer slag can have a unique effect on the enhancement of the fracture resistance of concrete.
5. The related tendency of the critical stress intensity factor (K^S_{IC}) of the slag concretes is similar to that of the fracture energy. At early ages (14 days), the K^S_{IC} values of slag concrete are less than that of the reference concrete (R0) but exceed that of R0 after 56 days.
6. Concretes incorporating finer slag exhibit larger K^S_{IC}, and the K^S_{IC} increases in conjunction with the fineness level of the slag. This also implies an increase in the fracture resistance of the concrete.

Author Contributions: Conceptualization, C.-H.W. and T.Y.; Methodology, C.-H.W.; Validation, C.-H.W., C.-H.H. and S.-K.L.; Formal analysis, C.-H.W. and C.-H.H.; Investigation, C.-H.W. and C.-H.H.; Resources, C.-H.W.; Data curation, C.-H.W. and S.-K.L.; Writing—original draft preparation, C.-H.W.; Writing—review & editing, C.-H.W. and T.Y.; Visualization, C.-H.W. and S.-K.L.; Supervision, T.Y.; Project administration, C.-H.H.

Funding: This research received no external funding.

Conflicts of Interest: The authors declare no conflict of interest.

References

1. Babu, K.G.; Kumar, V.S.R. Efficiency of GGBS in Concrete. *Cem. Concr. Res.* **2000**, *30*, 1031–1036. [CrossRef]
2. Mehta, P.K. Pozzolanic and Cementitious By-products as Mineral Admixtures for Concrete—A Critical Review. *Int. Concr. Abstr. Portal* **1983**, *79*, 1–46.
3. Malhotra, V.M.; Mehta, P.K. Pozzolanic and Cementitious Materials. In *Advances in Concrete Technology*; Gordon and Breach: London, UK, 1996.
4. Babu, K.G.; Kumar, V.S.R. Performance of GGBS in Cementitious Composites. In Proceedings of the Sixth NCB International Seminar on Cement and Building Materials, New Delhi, India, 24–27 November 1998; p. XIII-76.
5. Tan, K.; Pu, X. Strengthening Effects of Finely Ground Fly Ash, Granulated Blast Furnace Slag, and Their Combination. *Cem. Concr. Res.* **1998**, *28*, 1819–1825. [CrossRef]
6. Mantel, D.G. Investigation into the Hydraulic Activity of Five Granulated Blast Furnace Slags with Eight Different Portland Cements. *ACI Mater. J.* **1994**, *91*, 471–477.
7. Yűksel, I.; Özkan, Ö.; Bilir, I. Use of Granulated Blast Furnace Slag in Concrete as Fine Aggregate. *ACI Mater. J.* **2006**, *103*, 203–208.
8. Duan, P.; Shui, S.; Chen, W.; Shen, C. Effects of Metakaolin, Silica Fume and Slag on Pore Structure, Interfacial Transition Zone and Compressive Strength of Concrete. *Constr. Build. Mater.* **2013**, *44*, 1–6. [CrossRef]
9. Gao, J.M.; Qian, C.X.; Lin, H.F.; Wang, B.; Li, L. ITZ Microstructure of Concrete containing GGBS. *Cem. Concr. Res.* **2005**, *35*, 1299–1304. [CrossRef]
10. Chinaprasirt, P.; Homwuttiwong, S.; Sirivivantananon, V. Influence of Fly Ash Fineness on Strength, Drying Shrinkage and Sulfate Resistance of Blended Cement Mortar. *Cem. Concr. Res.* **2004**, *34*, 1087–1092. [CrossRef]
11. Zhu, J.; Zhong, Q.; Chen, F.; Li, D. Effect of Particle Size of Blast Furnace Slag on Properties of Portland Cement. *Procedia Eng.* **2012**, *27*, 231–236. [CrossRef]
12. Nadeau, J.C. A Multiscale Model for Effective Moduli of Concrete Incorporating ITZ Water-Cement Ratio Gradients, Aggregate Size Distributions and Entrapped Voids. *Cem. Concr. Res.* **2003**, *33*, 103–113. [CrossRef]
13. Hillerborg, A.; Modeer, M.; Petersson, P.E. Analysis of Crack Formation and Crack Growth in Concrete by Means of Fracture Mechanics and Finite Elements. *Cem. Concr. Res.* **1976**, *6*, 773–782. [CrossRef]
14. Petersson, P.E. *Crack Growth and Development of Fracture Zones in Plain Concrete and Similar Materials*; Rep. TVBM-1006; Division of Building Materials, Lund Institute of Technology: Lund, Sweden, 1981.
15. Hillerborg, A. The Theoretical Basis of a Method to Determine the Fracture Energy G_F of Concrete. *Mater. Struct.* **1985**, *18*, 291–296. [CrossRef]
16. Rao, G.A.; Raghu Prasad, B.K. Size Effect and Fracture Properties of HPC. In Proceedings of the 14th Engineering Mechanics International Conference (ASCE), Austin, TX, USA, 21–24 May 2000; p. 104.
17. Rao, G.A. Fracture Energy and Softening Behavior of High-Strength Concrete. *Cem. Concr. Res.* **2001**, *32*, 247–252. [CrossRef]
18. Surendra, P.S. Determination of the Fracture Parameters (K^S_{IC} and CTODC) of Plain Concrete Using Three-Point Bend Test. *Mater. Struct.* **1990**, *23*, 457–460.
19. Jenq, Y.S.; Shah, S.P. Two Parameters Fracture Model for Concrete. *J. Eng. Mech. ASCE* **1985**, *111*, 1227–1241. [CrossRef]
20. Jensen, E.A.; Hansen, W. Fracture Energy Test for Highway Concrete—Determining the Effect of Coarse Aggregate on Crack Propagation Resistance. *Transp. Res. Rec.* **2001**, *1730*, 10–16. [CrossRef]
21. RILEM Technical Committee 50-FMC, Proposed RILEM Recommendation. Determination of The Fracture Energy of Mortar and Concrete by Means of Three-Point Bend Tests on Notched Beams. *Mater. Struct.* **1985**, *18*, 285–290.
22. Giaccio, G.; Rocco, C.; Zerbino, R. The Fracture Energy (G_F) of High-Strength Concretes. *Mater. Struct.* **1993**, *26*, 381–386. [CrossRef]

23. Gettu, R.; Bažant, Z.P.; Karr, M.E. Fracture Properties and Brittleness of High-Strength Concrete. *ACI Mater. J.* **1990**, *87*, 608–617.
24. Xie, J.; Elwi, A.E.; MacGregor, J.G. Mechanical Properties of Three High-Strength Concretes Containing Silica Fume. *ACI Mater. J.* **1995**, *92*, 135–145.